Utilization of the cement industry CO_2 in the production of calcium carbonate nanoparticles through precipitation process intensification on a packed bed reactor

F. Liendo, F.A. Deorsola, S. Bensaid, G. Saracco

Department of Applied Science and Technology, Politecnico di Torino, 10129, Turin, Italy.

Corresponding author: Fabio A. Deorsola, e-mail address: fabio.deorsola@polito.it, tel.: +39 011 0904662, fax: +39 011 0904699

Abstract

This article presents an investigation on the recovery of CO_2 from flue gases of the cement industry through carbonation route in order to obtain calcium Carbonate Nanoparticles (CCnP), which are widely used as polymer and cement fillers. Two different experimental setups, a stirred tank reactor equipped with a sparger (named Bubbling Reactor, BR) and Packed Bed Reactor (PBR), were studied to improve the final product and enhance the process yield. The influence of the operating parameters on the particle size and morphology was tested for both reactors. The process was enhanced and intensified by employing the PBR, resulting in the synthesis of cubic calcite particles smaller than 300 nm and in higher CO_2 conversions with respect to the BR performance.

Keywords: calcium carbonate nanoparticles, process intensification, cement industry, CO_2 utilization.

1. Introduction

Nowadays, there are serious environmental issues of global warming, principally due to the Green House Gas (GHG) emissions, mainly carbon dioxide CO_2. Several industries can be considered responsible for the emission of these gases, such as cement, iron, steel, chemical, pulp, paper, aluminium and other industries. The cement industry is reported to produce about 25% of the global emissions of CO_2. Carbon footprint is equal to 680 kg CO_2 equivalent per cement ton. Several CO_2 capture, reuse and storages technologies have been developed, which involves physical, chemical and even biological process. Two categories of capture can be identified, namely pre and post combustion CO_2 capture. The first one refers to separation of CO2 generated as a co-product of a conversion process, while the last is based on solvents and solid sorbents. Despite all the effort on the part of researchers, many of these technologies do not come to be applied on an industrial scale. Although several absorption, adsorption, membrane and cryogenic methods have been developed, absorption processes are the most widely used in commercial applications [1]. The CO_2 capture technology to choose depends on its partial pressure in the flue stream. However, the GHG emissions are still too high and further researches need to be carried out in order to develop applicable technologies industrially for global warming mitigation.

Therefore, as objective of this study, the achievement of an added value product by the recovery of CO_2 from combustion gases of the cement industry was investigated. Calcium Carbonate Nanoparticles (CCnP) have been widely synthesized via carbonation route [2, 3, 4, 5, 6]. Ramakrishna, et al. produced microsized $CaCO_3$ particles starting from a $Ca(OH)_2$ slurry solution via carbonation route. Ulkeryildiz, et al. produced hollow nano calcite starting from a $Ca(OH)_2$ slurry, by employing a jet flow reactor where the precipitation zone was separated from the stabilitation zone in order to avoid agglomeration and growth phenomenas. Instead, Ryu, et al. synthesized microsized $CaCO_3$ particles starting for NH_4OH. Sun and coworkers, starting from a $CaCl_2$ solution, synthesized CCnP by employing an innovative rotating packed bed, where a simultaneous absorption of CO_2 and NH_3 absorption occurred.

In general, this approach involves a precipitation phenomenon driven by a reaction, in addition of a multiphase process, where there is an interaction between precipitation and mass transfer process. The mass transfer has a very important effect on the precipitation process, since the simultaneous crystal formation may occur in the bulk solution as well as in a thin interfacial region according to the gas absorption rate. Actually, the precipitation can take place in both zones, and then they can move into the other zone by action of the fluid in which they are contained, where they may grow further via precipitation. The nucleation and growth are influenced by the saturation level determined by Equation 1, where $a_{Ca^{2+}}$, $a_{CO_3^{2-}}$ and k_{sp} are the activity coefficient of calcium ions, carbonate ions and the solubility product of the $CaCO_3$.

Equation 1

$$S = \sqrt{(a_{Ca^{2+}} * a_{CO_3^{2-}})/k_{sp}}$$

The precipitated calcium carbonate has received much attention owing to its wide application in such industrial fields as paper, rubber, plastics, paint, etc. [7]. Currently, it is widely used as cement filler in order to decrease the product costs and to improve some of the mechanical properties of the composite materials [8, 9]. Thus, this CO_2 can be reused for the production of $CaCO_3$ via carbonation of a calcium solution in alkaline conditions to produce CCnP to be used as filler in the cement, thus contributing to CO_2 circular economy as indicated in Figure 1. There

are many waste minerals containing high CaO amounts, like wollastonite [10]. Therefore, in this work a carbonation process of a CaO slurry through two kind of reactors as synthesis route for the production of calcium carbonate nanoparticles was studied and enhanced.

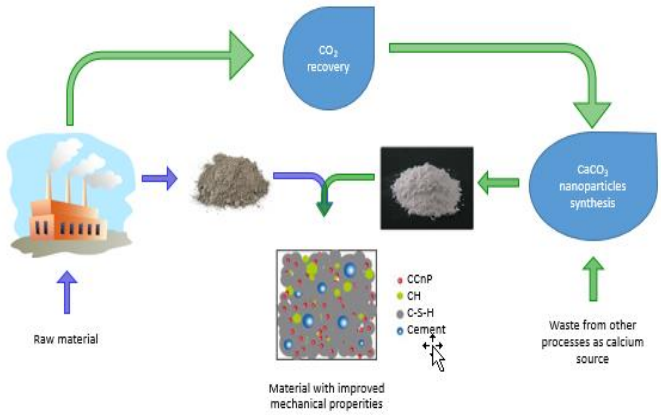

Figure 1. Circular economy process scheme of CO_2 reuse in the cement industry

1.1. $CaCO_3$ precipitation mechanism

Since calcium carbonate is sparingly soluble and its K_{ps} is equal to $4.4x10^{-9}$, it can be easily synthesizable by a precipitation method. Different calcium carbonate polymorphs can be obtained according to operating conditions. Calcite is the most stable calcium carbonate phase, while aragonite and vaterite are metastable and instable phases [11]. At higher temperatures, aragonite turns into more stable than the other calcium carbonate polymorphs [12, 13]. In Table 1 some properties of the anhydrous crystalline phases are summarized.

Table 1. Properties of the anhydrous crystalline phases [11, 12, 13]

Phase	**Crystallografic unit cell**	**Specific Gravity**	**Toughness**
Calcite	Hexagonal (rhombohedrical)	2.71 g/cm^3	Brittle
Vaterite	Hexagonal	2.65 g/cm^3	Brittle
Aragonite	Orthorombic	2.93 g/cm^3	Brittle

The $CaCO_3$ particles formation can follow the pathway hereafter described. In a saturated solution of Ca^{2+} and CO_3^{2-} ions (Equation 2), the precipitation reaction between them takes place. Then, calcium cations bond with carbonate ions forming calcium carbonate embryos in solution. The embryos grow to form a critical nucleus, which, if the local conditions are favourable, grows to form a primary nanoparticle [4]. As shown in normal conditions (Figure 2), three stages can be individuated. In the first stage, a prevalence of amorphous calcium carbonate can be observed. In the second stage, a coexistence of vaterite and calcite is present, while in the third and final stage calcite is practically the only phase present [14].

Equation 2

$$Ca^{2+}_{(aq)} + CO^{2-}_{3(aq)} \leftrightarrow CaCO_{3(s)} \downarrow$$

At the top left of Figure 3, the precipitation diagram of different calcium carbonate polymorph is shown [15]. As said before, calcite is the most stable polymorph at any temperature, since it has the lower solubility between the different calcium carbonate phases, given by its lower Activity Product (AP). So, hypothesizing a precipitation process of calcium carbonate, at the beginning of the process, with a high concentration of Ca^{2+} and CO_3^{2-} ions, supersaturation conditions for every phase are realized. The driving force for the nucleation is given by Equation 3. In the first stage of the calcium carbonate precipitation process, Amorphous Calcium Carbonate (ACC) is present in greater percentage. In the second stage, when the concentration gets lower, no more supersaturation conditions of ACC are present, and it gets dissolved again; because of this, in the second stage calcite and vaterite are present contemporaneously. At the end of the process, at lower concentrations, vaterite is no more saturated and it dissolves in solution again, giving just calcite presence at the end of the process [16, 17].

The transformation mechanism from ACC to the anhydrous crystalline polymorph can be related to the chemical composition of the local environment [16, 18]. That is, the synthesis method has an important role on the final properties of the calcium carbonate particles; principally, the operational parameters of the CO_2 bubbling lead to the synthesis of particles with different shape and size, but a poor control over the particle size distribution. Instead, through biomimetic methods and the use of apposite additives a better control over the particles' properties can be achieved [19].

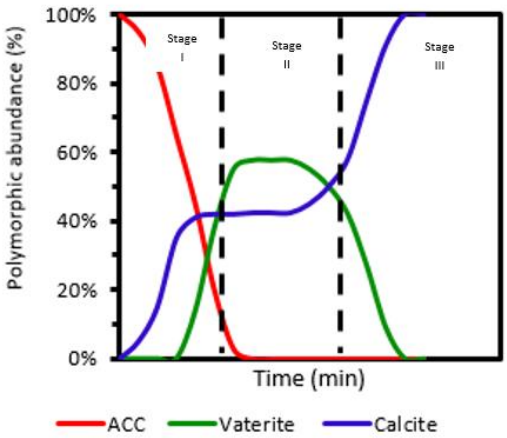

Figure 2. Change in Polymorphic abundance

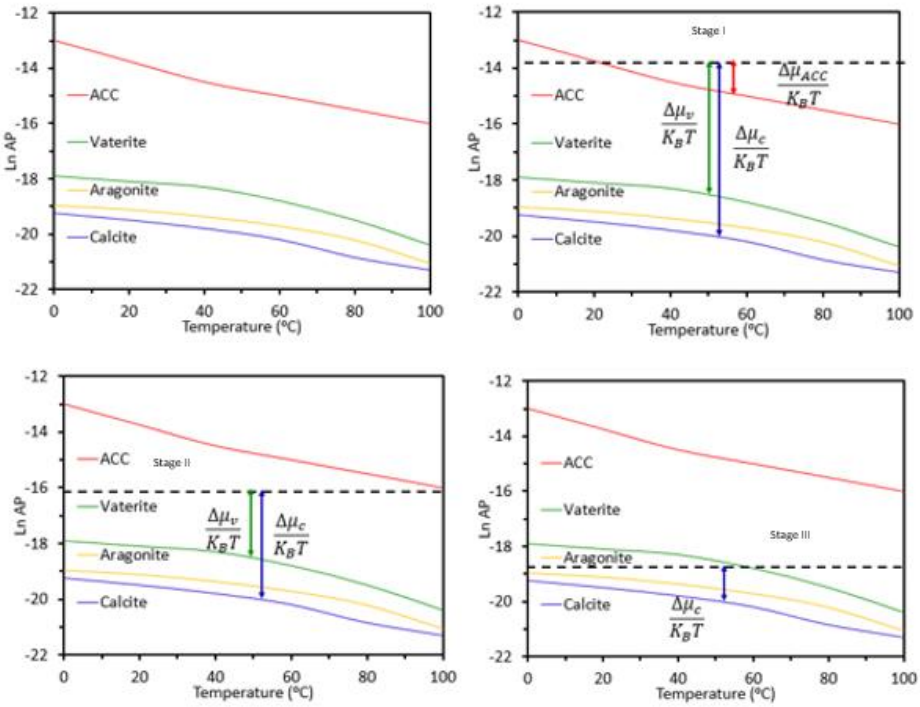

Figure 3. Calcium carbonate precipitation diagram [15]. a) I stage of the precipitation process, b) II stage, c) III stage.

Equation 3

$$\frac{\Delta\mu_i}{K_BT} = Ln\,AP - Ln\,K_i$$

where:
$\Delta\mu_i$ = Chemical Potential
K_B= Boltzmann Constant
T = Temperature
K_i= Activity product of the saturated state

Chemical reaction, nucleation and growth are the three main steps. In fact, they do not occur in this specific order but simultaneously, therefore it is worth to control these three steps during the precipitation. High degrees of supersaturation lead to the nucleation of small particles. By achieving high degrees of $CaCO_3$ supersaturation in the local sites, uniform spatial concentration distributions and identical growth time for all crystals, nano-$CaCO_3$ with narrow size distribution can be obtained. Macromixing and micromixing are occurring simultaneously in the reactors. Uniform spatial concentration distribution of any component on the vessel scale can only be achieved by macromixing, while uniform spatial concentration distribution on the molecular scale can only be reached by intense micromixing [20]. Hence, the CO_2 absorption mechanism takes a crucial role in the $CaCO_3$ particles

synthesis in order to obtain a high micromixing level. Micromixing is a key factor determining the degree of the supersaturation concentration of the solute and its local spatial distribution [3].

1.2. CO_2 absorption mechanism

Considering to employ a pure CO_2 cylinder (99.99%), the main resistance of the mass transfer is offered by the liquid phase, thus it controls the absorption process [21]. The liquid film is affected by different factors. In this case, a reactive absorption of CO_2 is considered, since it reacts with the OH^- ions according to the Equation 4 and Equation 5. The rate of carbon dioxide absorption could be considerably enhanced due to these fast reactions [21]. In this work, the effect of the effectiveness of the absorption process on the calcium carbonate precipitation was studied.

Equation 4: $$CO_2 + OH^- \leftrightarrow HCO_3^-$$

Equation 5: $$HCO_3^- + OH^- \leftrightarrow CO_3^{2-}$$

In a bubbling reactor (BR), illustrated in Figure 4a, the gas stream is fed to the reactor through the sparger at the bottom of the reactor, forming small or big bubbles according to the process conditions. The area of these bubbles influences, then, the mass transfer rate. Furthermore, in a BR, there many segregation problems, therefore, the supersaturation grade would not be homogeneous in the whole reactor, as illustrated in Figure 4a. Consequently, carrying out the precipitation process in a conventional apparatus, such as a stirred tank reactor, entails issues in controlling the quality of the product and the morphology as well as the size distribution of the particles often change from one batch to another [22, 3]. This is because of the poor micromixing present in this kind of reactors [3].

By employing a Packed Bed Reactor (PBR), this issue could be reduced and the micromixing enhanced by optimizing the operating conditions. In this kind of reactor, the liquid forms a layer over the packing, which has a thickness (δ) that depends on the flow regime of the process, as seen in Figure 4b. The flow regime has an important influence on the mass transfer coefficient. The film thickness plays a fundamental role: a thin film and sufficient turbulent conditions provide a uniform concentration on the vessel scale and molecular scale, by intense macro and micromixing, respectively, resulting in an enhanced CO_2 mass transfer and great increase of the nucleation rate [3]. By controlling these factors, small particles with a narrow particles size distribution were expected. The liquid flow effect on the film thickness have been widely studied [23, 24, 25]. These researchers performed the visual study of liquid flow in the PBR and established a model to represent the flow patterns, which indicated that the liquid in the packing existed as films attached to the packing wire and filling the voids of the packing. Zhao et al, concluded that three parameters have to be correlated to the experimental data: the relative thickness of the liquid (δ), the viscous effects (Re, Reynolds number) and the capillary effects (Ca, Capillary number) [25]. In addition, the study of the flow regime in concurrent gas-liquids upward flow through packed bed was performed by Murugesan et al [26], concluding that flow regime transitions and the frictional pressure drop are strongly influenced by all the fundamental as well as the operating variables of the system considered [26]. They developed a correlation for the estimation, according to the operating conditions, of the three different flow regimes in packed beds (bubble, dispersed bubble and pulse) which are considered in this work. These three different regimes have an influence on the mass transfer surface area and micromixing; hence, by controlling this, the absorption-precipitation process can be enhanced.

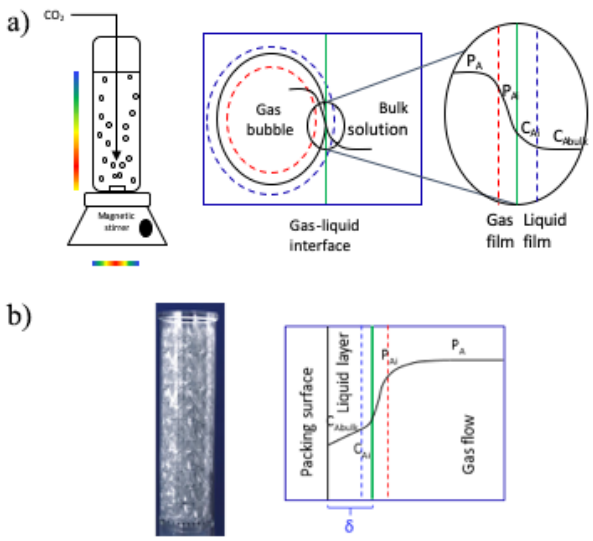

Figure 4. CO_2 absorption mechanism in both cases. a) Bubbling reactor. b) Packed bed reactor.

In the boundary phase region, different mechanisms take place after the carbon dioxide absorption, which could be considerably enhanced due to the fast reaction between carbon dioxide and hydroxyl ions (see Equation 4).This reaction, at the same time, is boosted by the subsequent reaction between bicarbonate ions and hydroxyl ones for the carbonate ions formation according to Equation 5. Then, the presence of Ca^{2+} ions triggers the precipitation of $CaCO_3$, according to Equation 2. The precipitation mechanism of $CaCO_3$ through a carbonation route could be affected respect to the described mechanism previously [16].
Following the described approach, this study concerns the increase of K_{La} and micromixing increasing through the implementation of the packed bed reactor, since higher turbulent conditions and mass transfer rates can be achieved than in a conventional bubbling reactor. Therefore, an increasing of the conversion of CO_2 from flue gas is expected, achieving thus the reduction of GHG emissions.

2. Materials and methods

2.1. Chemicals and synthesis method

$CaCO_3$ particles were synthesized through carbonation with pure CO_2 of a CaO slurry. Two different experimental setups were employed. The first one was a Bubbling Reactor (BR) with magnetic stirring, as simple and traditional option for the synthesis through carbonation route. Then an intensified option, a Packed Bed Reactor (PBR) filled with 5aschig rings as random packing, was employed for this study in the . In both cases, the synthesis was carried out at constant stirring and flowrates. The CO_2 flow was stopped once the pH was less than 10.5, value at which, according to the carbonate equilibria, the CO_3^{2-} formation is not favoured, thus reducing the $CaCO_3$ saturation. In the packed bed, two zones are individuated: *i*) the crystallization one inside the PBR itself, whence the CO_2 and the calcium solution get in contact and the precipitation takes place and *ii*) the stabilization one inside the feed tank, where the pH is maintained high enough to provide a stable environment for the $CaCO_3$ particles, since under alkaline conditions growth and agglomeration phenomena of the CCnP are not favoured [2]. The parameters of the PBR are summarized in
Table ***2***. Then, one the process was finished, the synthesized particles were immediately filtered by vacuum (pore size = 0.45 μm) and repeatedly washed with deionized water to eliminate ion excess. By last, the $CaCO_3$ powder was dried at 60 °C overnight and it was finally ready for characterization of their size, morphology and crystal phase.

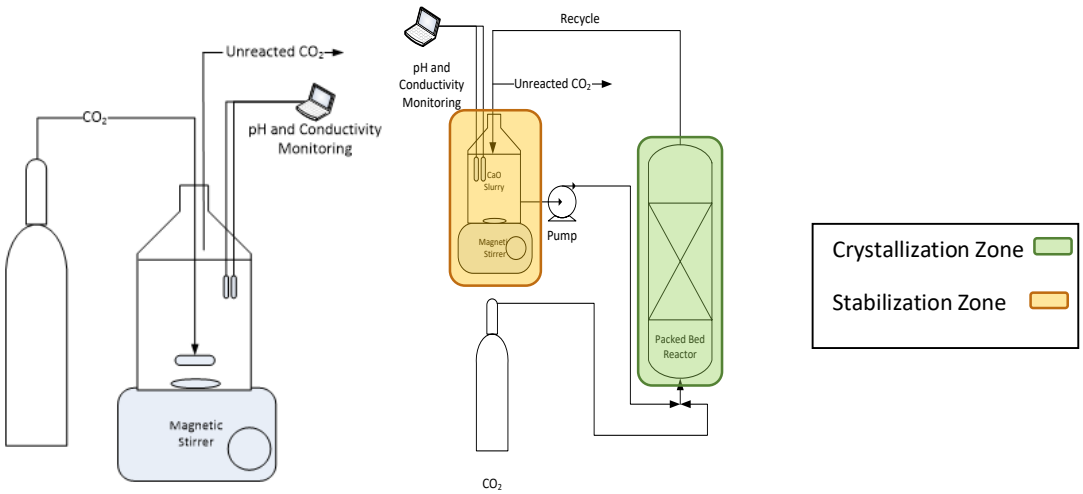

a) b)

Figure 5. Different experimental setup employed. A) Bubbling reactor b) Packed bed reactor.

Table 2. Packed bed reactor parameters.

System Parameters	
Length (mm)	370
Inner Diameter (mm)	10
Packing Surface Area (m^2/m^3)	1200
ε (m^3/m^3)	0.62

2.2. Particles characterization

Different characterization analyses were performed on the $CaCO_3$ powder. The dried powder was re-dispersed in isopropanol (0.5 g/L) and about 1 mL of sample was put into a UV cuvette for the measurement of size and size distribution by the dynamic light scattering (DLS) method using particle size analyser (Malvern nano ZS model). The phase purity of the samples was examined by X-Ray diffraction (Panalytical X'Pert Pro) in the 2θ range of 20-70° with a scanning step of 0.013° and a radiation CuKα, k = 1.54056 Å. The morphological characterization was obtained using field emission scanning electron microscopy (ZEISS MERLIN FE-SEM operated at 3 kV). The samples were prepared for electron microscopy observations by suspending a small quantity of nanoparticles in isopropanol, through ultrasonic mixing for 30 min, and subsequently by placing a drop of the dispersion on a copper grid coated with a layer of amorphous carbon.

3. Results and discussion

3.1. Bubbling Reactor (BR) performance

In the bubbling reactor, the effect of the initial calcium concentration and of the gas flowrate on the process and particles properties, such as size, morphology and crystalline phase was explored. The mass transfer coefficient was calculated according to correlations published by Levenspiel and Perry [27, 28], obtaining values of about 10^{-4} for any case of study, which are in good agreement with the values obtained through CFD simulations performed by different researchers [29, 30, 31] and with the experimental ones obtained by Alves et al. [32]. The different runs performed are summarized in Table 3.

Table 3. Run parameters of BR tests.

Run	Initial CaO concentration [mol/L]	Stirring velocity [rpm]	Gas flowrate [mL/min]
1	0.015	1200	100
2	0.015	1200	225
3	0.015	1200	380
4	0.015	1200	550
5	0.025	1200	225
6	0.05	1200	225

3.1.1. Effect of gas flowrate

Figure 6 shows the effect of the gas flowrate on the synthesis of $CaCO_3$ particles. The reaction temperature, the initial CaO concentration and the stirring velocity were, 20 (±1) °C, 0.015 mol/L and 1200 rpm, respectively. As can be appreciated in Figure 6a, for runs 1 and 2 the pH was maintained pretty constant during the beginning of the reaction, while the conductivity decreased linearly, which indicates the formation of the $CaCO_3$ according to Equation 2. The high pH provides stability to the formed particles and agglomeration and growth phenomena are disadvantaged [2, 9]. A high rate of CO_2 absorption led to lower synthesis time and a faster precipitation of the salt, then smaller particles would be obtained [3]. In fact, smaller particles were obtained for 225 mL/min (run 2) than for 100 mL/min (run 1), where a high synthesis time was obtained. Instead, for runs 3 and 4, where higher CO_2 flowrates were employed, both pH and conductivity decreased rapidly. This means that in these cases, the higher CO_2 flowrate led to a high rate of reaction of the OH^- ions according to Equation 4 than to Equation 5, meaning that the absorption rate is higher than the precipitation one. At this pH value, the precipitated particles are not very stable and tend to agglomerate and grow [9]. In fact, larger particles were obtained in these cases, for higher flowrates despite of their shorter synthesis time, as shown in Figure 6b.

It is important to note that the mean particle size is referred to a combination of primary particles, but also to the dimension of the different agglomerates. In fact, as seen in Figure 7, in the run 2 smaller particles were obtained but a wide Particle Size Distribution (PSD) can be observed, probably due to agglomeration phenomena, but also to heterogeneous process due to the segregation issues present in this kind of reactors, as shown in the CFD modulations carried out by Devi et al. [31]. Larger particles and wider PSD obtained with this reactor may be due to back-mixing and recirculation issues that led to poor mixing performance between reactants [33] and characteristic exponential residence time distribution of a CSTR [34]. Hence, the PSD is in good agreement to the FESEM micrograph, where cubic particles with different sizes are shown. This is the classical morphology of calcite, which is the only crystalline phase present according to the XRD spectra shown in Figure 7. Furthermore, the calcite crystalline phase was not affected by the gas flowrate.

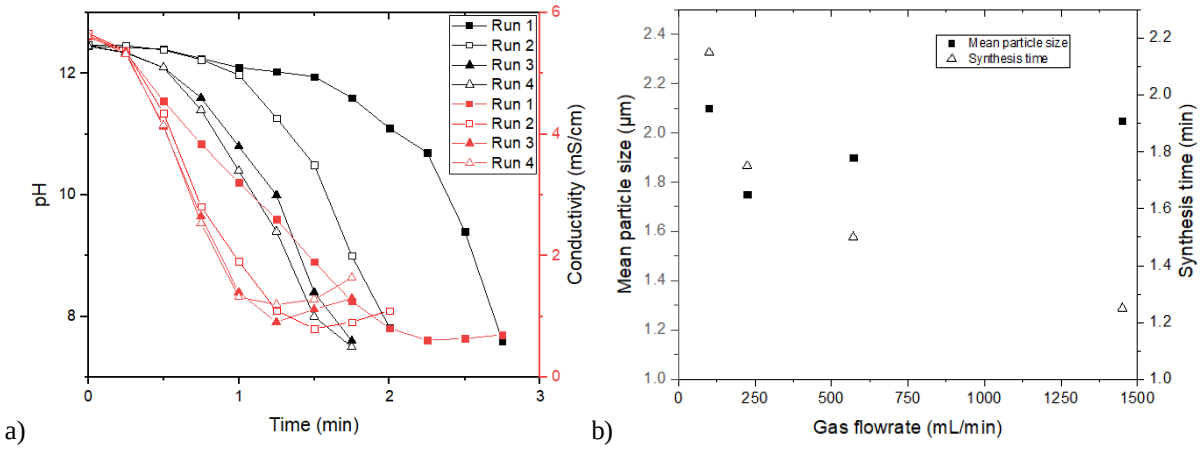

Figure 6. Gas flowrate effect on $CaCO_3$ particles synthesis by BR alternative. a) Effect on the ab sorption kinetics. b) Effect on mean particle size.

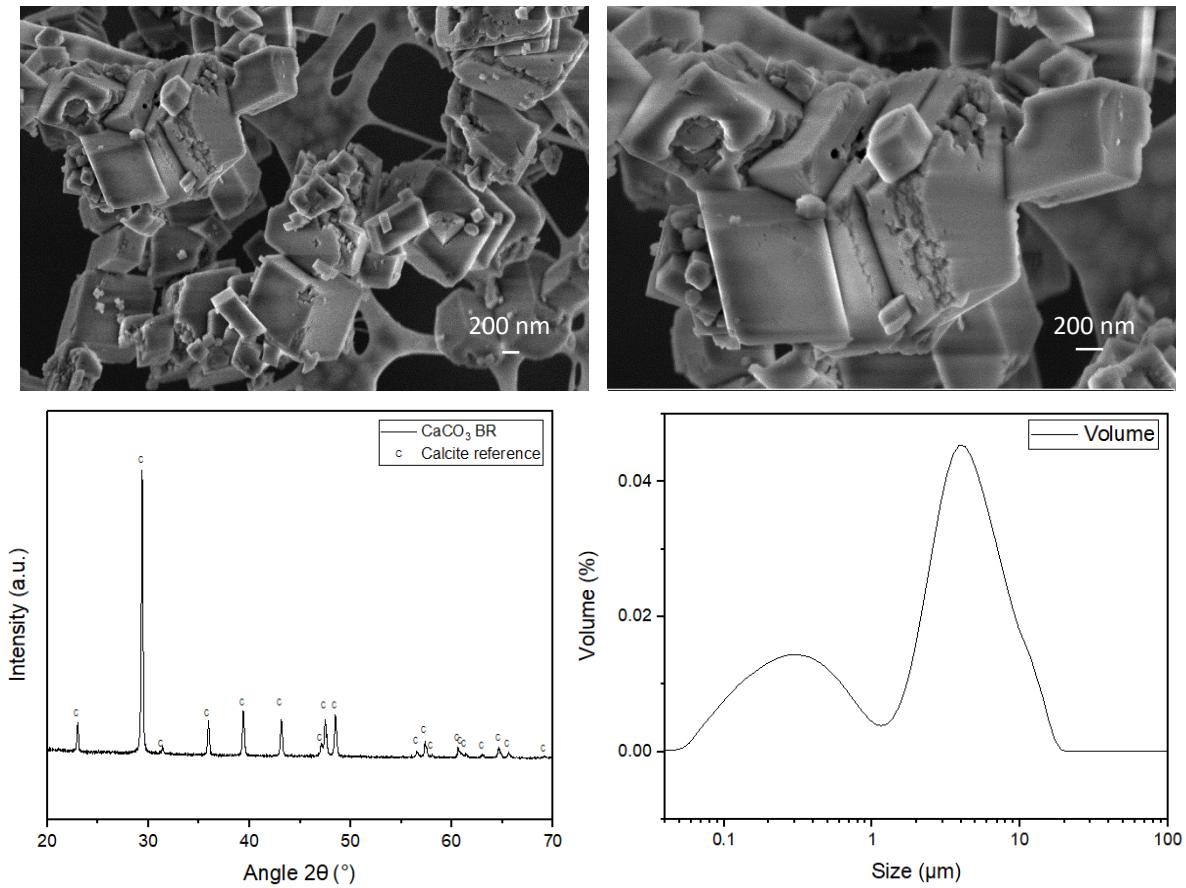

Figure 7. *$CaCO_3$ particles synthesized according to the operation parameters in run 2.*

3.1.2. Effect of initial CaO concentration

By maintaining constant temperature, gas flowrate and stirring speed, equal to 20 (±1) °C, 225 mL/min and 1200 rpm respectively, the effect of the initial calcium oxide concentration on the $CaCO_3$ synthesis was studied. Three different concentrations were studied, 0.015, 0.025 and 0.05 mol/L. The initial CaO concentration had no any effect on the crystalline phase; as in the case of the study of the gas flowrate, just calcite was obtained for each CaO concentration. This fact is due that, as said before, calcite is the most stable polymorph of $CaCO_3$ [4, 16, 15], and since there is not any presence of extraneous ions or compound that can stabilize other polymorph form [4, 16, 35, 19, 36], the formation of calcite was always favored.

Figure 8 shows that an increment of the initial CaO concentration bring the system towards longer synthesis times despite of a higher concentration of the oxide means a more elevated pH. Therefore, the rate of transformation of CO_2 and HCO_3^- ions to the formation of CO_3^{2-} ions, according to Equation 4 and Equation 5, is enhanced by the higher concentration of OH^- ions. This is due to the fact that the $CaCO_3$ precipitation rate is almost constant and it

is practically independent on the calcium concentration. As in the previous case, longer synthesis times led to the production of larger particles.

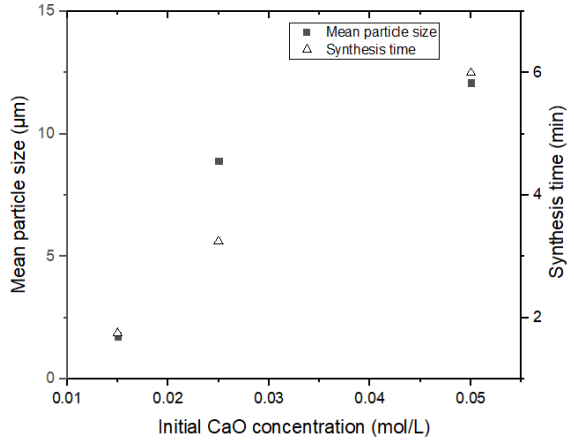

Figure 8. Initial CaO concentration on $CaCO_3$ particles synthesis by BR alternative.

3.2. Packed Bed Reactor (PBR) performance

In the packed bed reactor, in addition to the study of the effect of the initial calcium concentration and the gas flowrate on the process and on the particles' properties, the effect of the liquid flowrate was also tested. The mass transfer coefficient was calculated according to correlations published by researchers [37], obtaining values of about 10^{-3}-10^{-2} for any case considered. This means an improvement in the mass transfer coefficient. Consequently, segregation and polydispersity issues presented in the BR are expected to be reduced. The different runs are summarized in Table 4.

Table 4. Run parameters of PBR tests.

Run	Initial CaO concentration (mol/L)	Gas flowrate (mL/min)	Liquid Flowrate (mL/min)
7	0.015	100	108
8	0.015	225	108
9	0.015	571	108
10	0.015	1450	108
11	0.015	1450	250
12	0.015	1450	350
13	0.015	1450	400
14	0.025	225	108
15	0.05	225	108

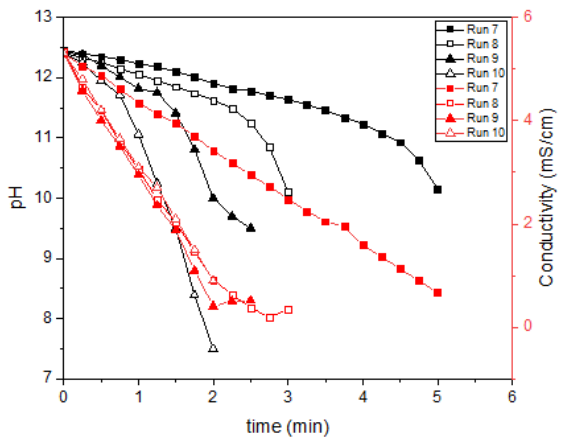

a)

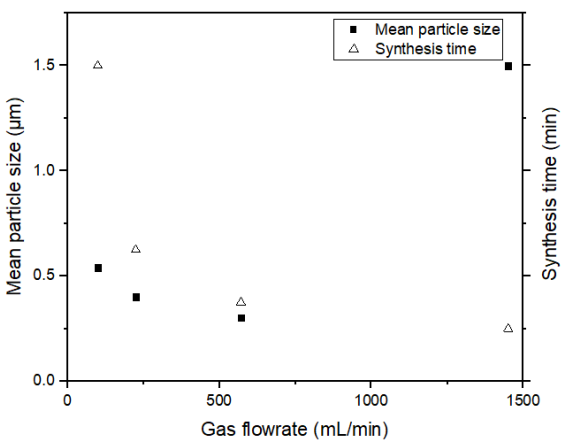

b)

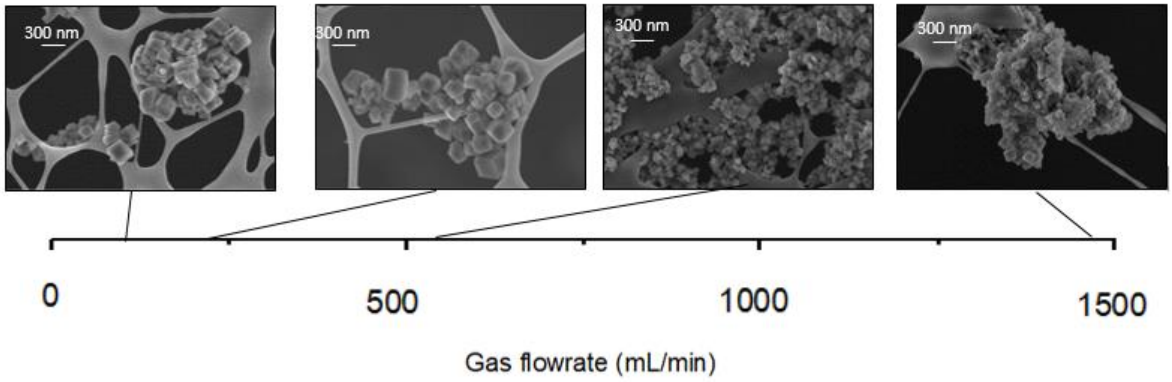

c)

Figure 9. Gas flowrate effect on $CaCO_3$ particles synthesis by PBR alternative. a) Effect on the absorption kinetics. b) Effect on mean particle size. c) Effect on morphology.

3.2.1. Effect of gas flowrate

Figure 9 shows the effect of the gas flowrate on the synthesis of the particles. For these tests, the reaction temperature, liquid flowrate, initial CaO and the stirring velocity were 20 (±1) ° C, 108 mL/min, 0.015 mol/L and 1200 rpm, respectively. Figure 9a shows that the reduction of the pH is faster by increasing the gas flowrate, therefore, the rate of formation and the subsequent consumption of CO_3^{2-} ions due to $CaCO_3$ precipitation, according to Equation 4, Equation 5 and Equation 2, were higher. The increase of the precipitation rate can be appreciated by the increasing of the slope in the conductivity vs time curve, which indicates the consumption of the Ca^{2+} ions. Therefore, the higher final conductivity by increasing the gas flowrate indicates that the conversion is lower by increasing the gas flowrate, despite of the higher absorption and precipitation rates. That is due that, after a pH value lower than 10.5 is reached, the CO_3^{2-} is no more favored; in fact, a plateau is seen at the end of the reaction, thus indicating the end of the synthesis. In such way, by increasing the gas flowrate the synthesis time was reduced, as seen in Figure 9b.

The mean particle size, determined by the DLS measurements and the FESEM images, is also shown in Figure 9b. The particle size was reduced by increasing the gas flowrate, but for the highest flowrate (1450 mL/min) the DLS measurements indicated microsized particles (1.5 μm). This value corresponds to the size of the aggregated primary particles, which had nanometric dimensions, as seen in the corresponding FESEM micrograph. The formation of these aggregates was probably due to the fast pH reduction and consequently instability of $CaCO_3$ particles [2, 9]. In all cases, cubic calcite particles were obtained, i.e. the gas flowrate had no effect on the polymorphism of the particles.

3.2.2. Effect of liquid flowrate

By maintaining temperature, gas flowrate, initial CaO concentration and stirring speed constant, equal to 20 (±1) ^oC, 225 mL/min, 0.015 mol/L and 1200 rpm respectively, the effect of the liquid flowrate on the $CaCO_3$ synthesis was studied. In this case, higher liquid flowrates led to maintain a higher pH during the synthesis, as shown in Figure 10a. Higher flowrates led to higher precipitation rates and calcium conversions according to the conductivity vs time curve. Anyway, a different precipitation mechanism can be supposed, since at higher liquid flowrates both cubic and laminated cubic particles were present, as seen in Figure 10b. In fact, the presence of laminated cubic particles was more evident by increasing the liquid flowrates. This was probably due to different flow regimes at these conditions, therefore the micromixing was surely affected and the growth phenomenon was favored over the nucleation one.

3.2.3. Effect of initial CaO concentration

By maintaining temperature, gas, liquid flowrate and stirring speed as constant, equal to 20 (±1) ^oC, 225 mL/min, 108 mL/min and 1200 rpm respectively, the effect of the initial calcium oxide concentration on the $CaCO_3$ synthesis was studied. Three different concentrations were studied, specifically 0.015, 0.025 and 0.05 mol/L. The initial CaO concentration had not any effect on the crystalline phase, as in the case of BR, and just calcite was obtained for each CaO concentration. Figure 11 shows that an increment of the initial CaO concentration had the same effect of the case of the BR, meaning that higher CaO concentrations led to longer synthesis times and larger particles.

Therefore, the conditions corresponding to run 9 (see Table 4) were determined as optimal conditions and the characterization of these particles is presented in Figure 12. PSD shows nanosized particles with a mean particle size equal to 300 nm, which is not in good agreement to the FESEM micrograph, where cubic primary calcite particles with sizes between 40-200 nm are shown. This is probably because the DLS measurements take into account the agglomerates size and not the primary particles one. Instead, the FESEM micrographs are in good agreement to the XRD spectra, where just presence of calcite as crystalline phase was determined.

3.3. Reactors comparison

The performance of both reactors was studied and compared by varying the gas flowrate and maintaining constant the temperature, concentration of CaO, stirring velocity and liquid flowrate in the case of the PBR equal to 20 (±1) °C, 0.015 mol/L, 1200 rpm and 225 mL/min, respectively. By employing the PBR, the synthesis of $CaCO_3$ through carbonation method was improved respect to the BR performance. Figure 13a shows that there was an intensification regarding the mean particle size, since an enhancement from synthesizing micro and polydispersed particles to producing dispersed nanosized cubic calcite particles was observed. This can be associated to the higher mass transfer coefficients provided by the PBR and, consequently, micromixing shorter times. Shorter micromixing times mean higher nucleation rates over growth [3] [38] [39]. Micromixing has an important effect on the particle size distribution, since a poor micromixing leads to highly nonlinear nucleation and growth kinetics of crystals. If micromixing time is too high, the nucleation and growth of crystals had already begun before micromixing in the precipitator was complete. As a consequence, the poor micromixing present in the BR led to supersaturation gradients present in the nonhomogeneous mixture resulting in a much wider particle size distribution [38, 40, 41]. In addition to the production of smaller filler particles, even higher conversions of calcium and CO_2 were reached by employing the PBR, as seen in Figure 13b. The higher mass transfer coefficients reached with this kind of setup led to a more sustainable precipitation process.

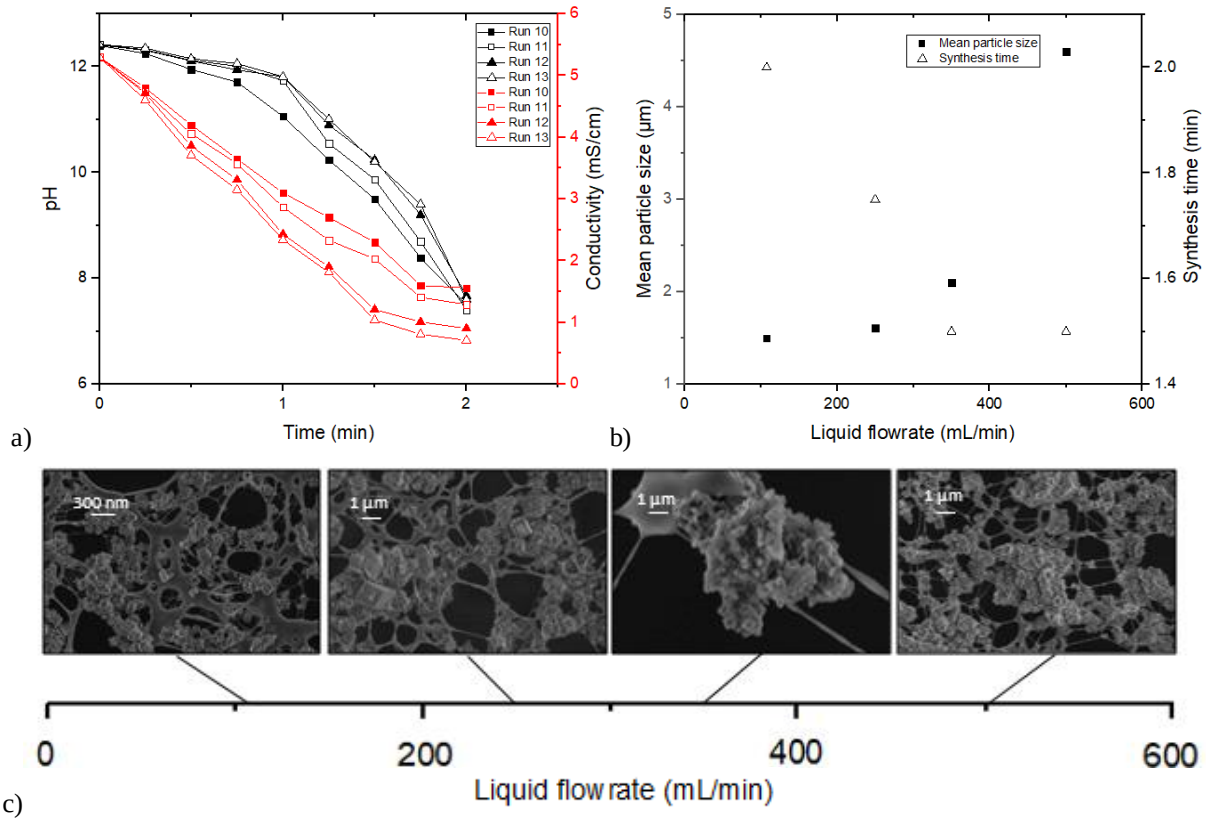

Figure 10. Liquid flowrate effect on $CaCO_3$ particles synthesis by PBR alternative. a) Effect on the absorption kinetics. b) Effect on mean particle size. c) effect on morphology.

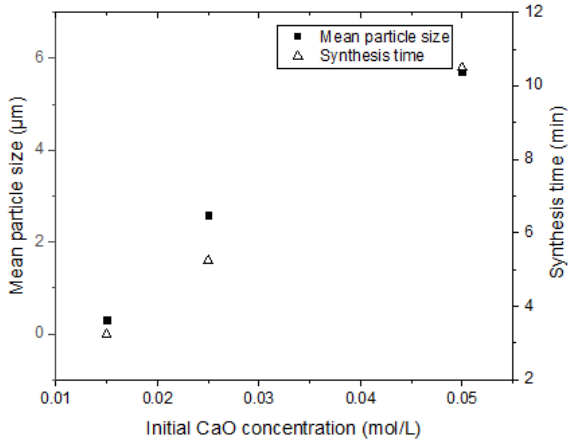

Figure 11. Initial CaO concentration on $CaCO_3$ particles synthesis by PBR alternative.

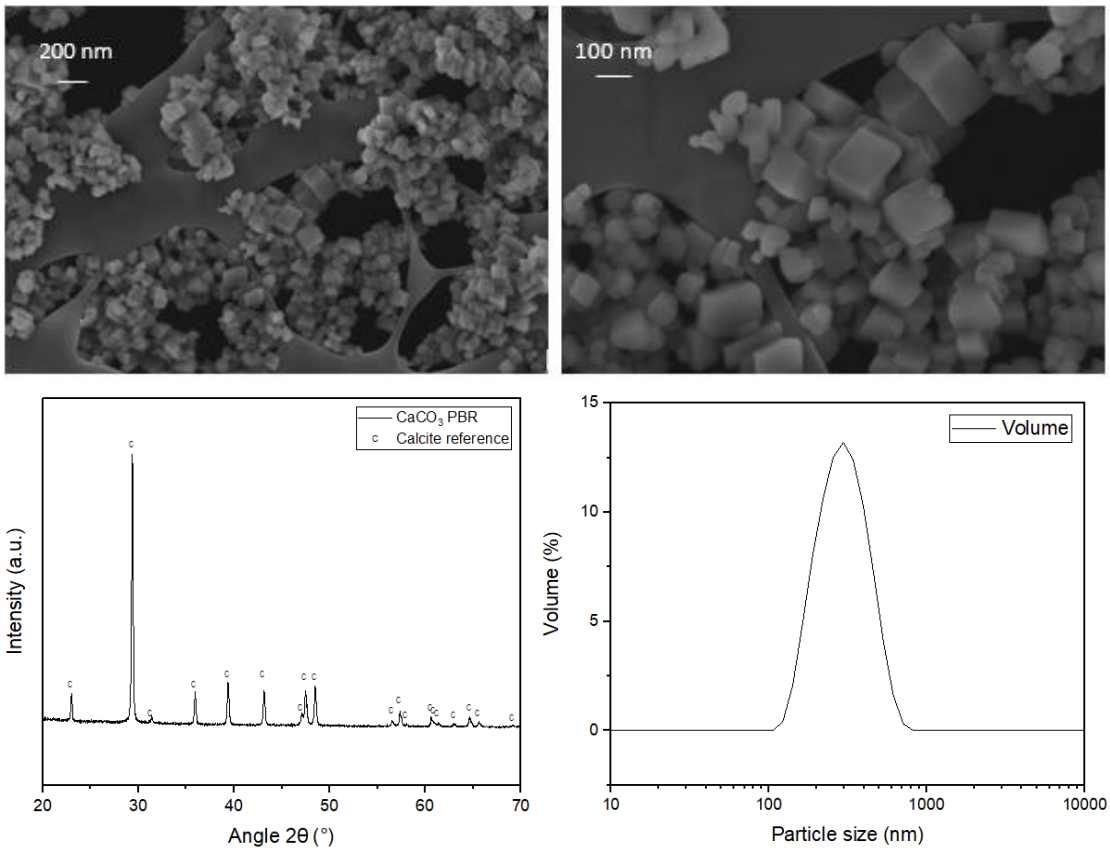

Figure 12. $CaCO_3$ particles synthesized according to the operation parameters in run 9.

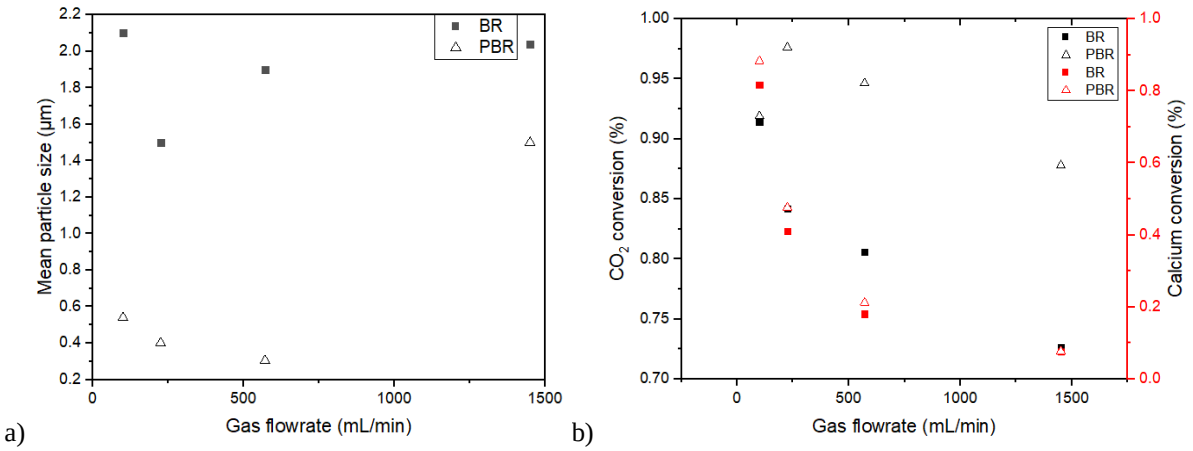

a) b)

Figure 13. Reactors performance comparison. a) Mean particle size by varying the gas flowrate. b) Calcium and CO_2 conversions on both alternatives, BR and PBR.

4. Conclusions

An intensification process was carried out, by employing a packed bed reactor (PBR) setup for producing $CaCO_3$ nanoparticles through a carbonation route. The preliminary issues presented by a bubbling reactor (BR) were reduced by maximizing the effectiveness of intra-and intermolecular events, that is enhancing the macro and micromixing. Thus, the same processing experience was given to each molecule in order to obtain a product with uniform properties. Microsized particles with a wide PSD were synthesized with the BR. On the other hand, the PBR provided a growth and agglomeration control at optimum conditions that led to synthesize nanosized particles with a narrow PSD. By this way, the conventional process has been enhanced in an intensified process, where nanosized calcite cubic particles were synthesized with an increase on process conversions in terms of calcium and CO_2.

Acknowledgements
This project has received funding from the European Union's Horizon 2020 research and innovation program under grant agreement 768583– RECODE (Recycling carbon dioxide in the cement industry to produce added-value additives: a step towards a CO2 circular economy) project. (https://www.recodeh2020.eu/).

References

[1] C. B. E. K. Efthymia Ioanna Koytsoumpa, "The CO2economy: Review of CO2capture and reuse technologies," *The Journal of Supercritical Fluids,* vol. 132, pp. 3-16, 2018.

[2] S. K. E. O. Eda Ulkeryildiz, "Nano-CaCO3synthesis by jet flow," *Colloids and Surfaces A: Physicochemical and Engineering Aspects,* pp. 34-40, 2016.

[3] X.-M. W. J.-M. C. G.-W. C. J.-F. C. L. S. Bao-Chang Sun, "Synthesis of nano-CaCO3 by simultaneous absorption of CO2 and NH3 into CaCl2 solution in a rotating packed bed," *Chemical Engineering Journal,* p. 731–736, 2011.

[4] E. R. a. O. M. S. A. Declet, "Calcium carbonate precipitation: a review of the carbonate crystallization process and applications in bioinspired composites," *Adv. Mater. Sci.,* pp. 87-107, 2016.

[5] T. T. a. J. W. A. Chilakala Ramakrishna, "Evaluation of Various Synthesis Methods for Calcite-Precipitated Calcium Carbonate (PCC) Formation," *Korean Chem. Eng. Res.,* vol. 55, no. 3, pp. 279-286, 2017.

[6] K. S. Y. J. W. A. a. H. K. Mi Young Ryu, "Effect of the pH and Basic Additives on the Precipitation of Calcium Carbonate during Carbonation Reaction," *Resources Processing,* vol. 54, pp. 14-18, 2007.

[7] L. X. Y. J. Y. Wen, "Synthesis of plate-like calcium carbonate via carbonation route," *Materials Letters* , vol. 57, pp. 2565-2571, 2003.

[8] J. K. M. N. L. Rieger, "Formation of nanoparticles and nanostructures-an industrial perspective on CaCO3, cement, and polymers," *Angewandte Chemie - International Edition,* pp. 12380-12396, 2014.

[9] G. T. E. O. Sevgi Kilic, "Stability of CaCO3 in Ca(OH)2 solution," *International Journal of Mineral Processing,* vol. 147, pp. 1-9, 2016.

[10] T. C. Clive Maier, "Fillers and reinforcements," in *Polypropylene,* 2008, pp. 49-56.

[11] K. P. A. M. a. R. J. R.S. Somani, *Industrial & Engineering Chemistry Research,* vol. 45, p. 5223, 2006.

[12] A. L. a. M. Meyers, *Materials Science and Engineering A,* 2005.

[13] D. Ming, *Encyclopedia of Soil Science,* 2006.

[14] *Pure & Appl. Chem.921-928, 1997,* vol. 69, pp. 921-928, 1997.

[15] N. S. A. M. a. M. K. 2. Jun Kawano, "Precipitation diagram of calcium carbonate polymorphs: its construction and significance.," *J. Phys.: Condens. Matter,* vol. 21, 2009.

[16] A. G. S. M. N. H. J. D. Y. P. D. C.R. Blue, "Chemical and physical controls on the transformation of amorphous calcium carbonate into crystalline CaCO3 polymorphs," *Geochimica et Cosmochimica Acta,* vol. 196, pp. 179-196, 2017.

[17] K. Sawada, "The mechanisms of crystallization and transformation of calcium carbonates," *Pure & Appl. Chem,* vol. 69, no. 5, pp. 921-928, 1997.

[18] Z. A. a. R. W. Zuhl, "Calcium carbonate precipitation in presence of inhibitors," *Materials performance,* pp. 42-47, 2007.

[19] V. K. P. a. J. L. Yash Boyjoo, "Synthesis of micro and nano-sized calcium carbonate particles and their applications," *J. Mater. Chem. A.,* vol. 2, pp. 14270-14288, 2014.

[20] L. S. J.F. Chen, "Mass production of nanoparticles by high gravity reactive," *China Particuol,* vol. 1, pp. 64-69, 2003.

[21] Y. T. A. Tamir, "The effect of the gas side resistance on absorption with chemical reaction from binary mixtures," *Chemical Engineering Science,* vol. 30, pp. 1477-1482, 1975.

[22] L. S. J.-F. C. Hong Zhao, "High-gravity process intensification technology and application," *Chemical Engineering Journal,* pp. 588-593, 2010.

[23] A. a. H.-J. B. Ataki, "The use of the VOF-model to study the wetting of solid surfaces," *Chem. Eng. Technol.,* pp. 1109-1114, 2004.

[24] A. a. H.-J. B. Ataki, "Experimental and CFD simulation study for the wetting of a structured packing element with liquids," *Chem. Eng. Technol.,* vol. 29, no. 3, pp. 336-347, 2006.

[25] L. Z. a. R. L. Cerro, "EXPERIMENTAL CHARACTERIZATION OF VISCOUS FILM FLOWS OVER COMPLEX SURFACES," *Int. J. Multiphase Flow,* vol. 19, no. 4, pp. 495-516, 1992.

[26] V. S. T. Murugesan, “Pressure drop and flow regimes in cocurrent gas–liquid upflow through packed beds,” *Chemical Engineering Journal,* vol. 88, pp. 233-243, 2002.

[27] O. Levenspiel, Chemical reaction engineering, John Wiley & Sons, 1999.

[28] R. H. Perry, Perry's Chemical Engineers' Handbook, 7th ed., McGraw-Hill, 1997.

[29] S. S. Ranganathan P., “Investigations on hydrodynamics and mass transfer in gas–liquid stirred reactor using computational fluid dynamics,” *Chemical Engineering Science,* vol. 66, no. 14, pp. 3108-3124, 2011.

[30] L. V. E. K. R. J. F. F. M. Moucha T., “Improved power and mass transfer correlations for design and scale-up of multi-impeller gas-liquid contactors,” *Chemical Engineering Science,* vol. 64, no. 3, pp. 598-604, 2009.

[31] B. K. T. Devi, “Mass transfer and power characteristics of stirred tank with Rushton and curved blade impeller,” *Engineering Science and Technology, an International Journal,* vol. 20, no. 2, pp. 730-737, 2017.

[32] C. M. J. V. S.S. Alves, “Experimental and modelling of gas dispersion in double turbine stirred tank,” *Chemical Engineering Journal,* vol. 89, no. 1-3, pp. 109-117, 2002.

[33] V. K. R. Wasique H. Khan, “Process intensification approach for preparation of curcumin nanoparticles via solvent-nonsolvent nanoprecipitation using spinning disc reactor,” *Chemical Engineering and Processing: Process Intensification,* vol. 80, pp. 1-10, 2014.

[34] D. A. P. J. a. W. Ray, “Tubular reactors for emulsion polymerization: I. Experimental investigation,” *AlChe Journal ,* vol. 40, no. 1, pp. 73-87, 1994.

[35] G. F. L. B. Ž. S. a. D. K. Branka Njegić-Džakula, “Effects of Initial Supersaturation on Spontaneous Precipitation of Calcium Carbonate in the Presence of Charged Poly-L-amino Acids”.

[36] J. Z. H. T. a. U. B. Qiaona Hu, “Growth process and crystallographic properties of ammonia-induced vaterite.,” *American Mineralogist,* p. 1437–1445, 2012.

[37] B. F. A. Y. T. Shah, “Gas-liquid mass transfer coefficients for cocurrent upflow in packed beds — Effect of packing shape at low flow rates,” *The Canadian Journal of Chemical Engineering,* vol. 54, no. 6, 1976.

[38] C. Z. a. G. C. Jianfeng Chen, “Interaction of macro and micromixing on particle size distribution in reactive precipitation,” *Chemical engineering science ,* vol. 51, no. 10, pp. 1957-1966, 1996.

[39] N. Tavare, “Mixing, reaction, and precipitation: Interaction by exchange with mean micromixing models,” *AIChE Journal,* pp. 2537-2548, 1995.

[40] S. R. a. J. B. R. Phillips, “Micromixing in a Single-Feed Semi-Batch precipitation process,” *AlChe Journal,* vol. 45, no. 1, pp. 82-92, 1999.

[41] A. J. M. a. D. J. Kinvan, “Micromixing Effects in a Two-Impinging-Jets Precipitator,” *AlChe Journal,* vol. 42, no. 7, pp. 1801-1814, 1996.